Liquid Crystalline Poly(vinyl ether)s with Bulk Smectic C* Phases at the Air/Water Interface

H. Fadel,[†] V. Percec,[‡] Q. Zheng,[‡] R. C. Advincula,[†] and R. S. Duran[*,†]

Center for Macromolecular Science and Engineering and Department of Chemistry, University of Florida, Gainesville, Florida 32611, and Department of Macromolecular Science, Case Western Reserve University, Cleveland, Ohio 44106

Received September 15, 1992; Revised Manuscript Received December 3, 1992

ABSTRACT: Monolayer behavior of a series of ferroelectric liquid crystalline polymers containing amphiphilic side groups has been investigated at the air/water interface using the Langmuir trough Surface pressure vs surface area isotherms measured as a function of temperature and barrier speed showed that the molecular assembly in the monolayer was dominated by packing of the mesogens. Surface potential vs surface area isotherms were performed to investigate dipole orientation and solvation effects during compression. Isobaric creep and hysteresis measurements indicated that these polymers are good candidates for transfer to solid substrates.

Introduction

To date many low molecular weight organic materials showing ferroelectric switching have been extensively studied with respect to their synthesis and physical properties.[1-13] However, ferroelectric liquid crystalline (LC) polymers presenting a smectic C* (s_{C^*}) phase are less investigated,[14-32] though of interest because of their high mechanical and thermal stability compared to low molecular weight compounds and their electrooptical properties.[33,34] Furthermore, by synthesizing low molecular weight polymers with defined polydispersities, many of these properties can be tailored in a rational manner. Mesogens in the bulk Sc* phase are well organized in layers, and they are tilted by a defined angle from the normal. A macroscopic cross section of these layers can be considered as analogous to an assembly of two-dimensional layers with a slight twist imposed between each layer.

It would then be of interest to study the physical properties of molecules which show this type of bulk organization when the molecules are confined to a single layer in a measurable two-dimensional scale. By spreading the molecules at an air/water interface, they are forced to form a monolayer confined to an experimentally-defined two-dimensional scale, yet they are free to reorient laterally due to the liquid nature of the substrate. This type of ordering, when the molecules are close packed, may be compared to a single smectic layer ordering in the bulk with additional tilt orientational order imposed by the amphiphilic character of the side chains. By changing the applied surface pressure, the mesogenic tilt angle may, in principle, be varied over a wide range. Thus the behavior of ferroelectric liquid crystalline polymers confined to monolayers at a free surface may provide valuable insights into bulk behavior. This kind of study is made possible by the Langmuir–Blodgett technique and is the topic of the present work.

An additional interest in Langmuir film formation[35,36] lies in the possibility of producing an assembly of highly-ordered multilayers deposited on a solid substrate by dipping. In this manner, thin films with defined structure, chemical composition, and thickness can be prepared and investigated on a variety of different substrates. This kind of multilayer ordering can reduce defects compared to the bulk and can enhance the film properties. Model samples can also be prepared to investigate the effects of various molecular stacking sequences on phase behavior and switching,[37] for example.

We are interested in studies leading to better understanding of the physical properties of liquid crystalline (Sc*) forming substances at the air/water interface, specifically the influence of chemical structure and molecular architecture on monolayers of these materials. In previous studies, we investigated a series of LC polymers having the same mesogenic unit but different spacer lengths and copolymers.[38-40] We have also investigated the effect of molecular architecture on the morphology of the spread monolayer[41] and the viscoelastic properties of spread monolayers in the collapse region.[42]

In this work, the monolayer behavior of a series of three polymers having the same polymer backbone and different side groups is compared. The chemical structures of the polymers investigated are shown in Scheme I. All three polymers contained a poly(vinyl ether) backbone and showed enantiotropic s_{C^*} phases in the bulk.[43-45] The bulk thermal phase behavior is shown in Table I; the polymers will be referred to in the text by the abbreviations in Scheme I. The bulk transition temperatures shown in Table I reveal different disordered smectic LC phase transitions in a temperature range near ambient. This fact makes these compounds suitable for an analytical study on the Langmuir–Blodgett trough, where the temperature range is limited to temperatures below 50 °C. Further details of the synthesis of the polymers investigated are described below.

Experimental Section

All three polymers were synthesized by living cationic polymerization initiated by a $CF_3SO_3H/S(CH_3)_2$ system in CH_2Cl_2 at 0 °C. The resulting polymers are characterized by a combination of techniques consisting of gel permeation chromatography (GPC), differential scanning calorimetry (DSC), and thermal optical polarized microscopy. Scheme I illustrates the structures of the resulting polymers and their relative number-average molecular weights (relative to polystyrene standards), degrees of polymerization, and polydispersities. The molecular weights of these polymers were controlled by the monomer to initiator ratio ($[M]_0/[T]_0$), and the polydispersities were ≤ 1.11. More complete characterization is described elsewhere.[43-45]

The spreading solutions were prepared in spectrograde chloroform (Kodak) with a concentration between 0.5 and 1 mg/mL. All monolayer behavior studies were performed using a KSV 5000 Langmuir–Blodgett system (KSV Instruments) under a HEPA filter hood (Baker Co.). A two-barrier symmetric com-

---

[†] University of Florida.

[‡] Case Western Reserve University.

0024-9297/93/2226-1650$04.00/0

Scheme I
Poly[(*S*)-(−)-2-methylbutyl 4′-[[8-(vinyloxy)octyl]oxy]biphenyl-4-carboxylate] (C8/C*), Poly[2*S*,3*S*)-(+)-2-chloro-3-methylpentyl 4′-[[8-(vinyloxy)octyl]oxy]biphenyl-4-carboxylate] (C8/C), and Poly[(2*S*,3*S*)-(+)-2-chloro-3-methylpentyl 4′-[[6-(vinyloxy)hexyl]oxy]biphenyl-4-carboxylate] (C6/C**)**

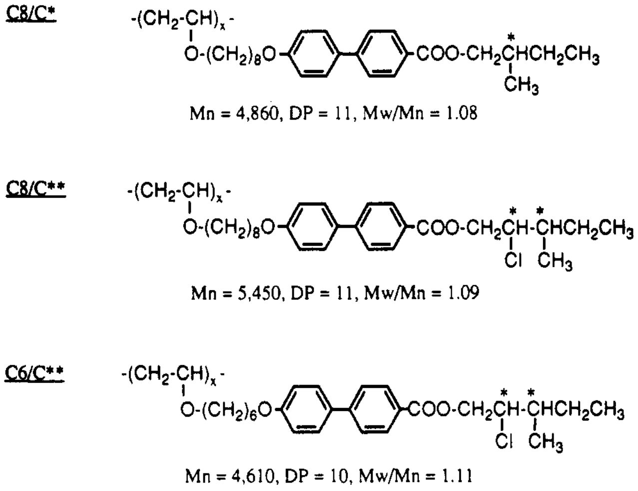

Table I
Thermal Transition Temperatures (°C) and Corresponding Enthalpy Changes (kcal/mru)[a]

C8/C*	g 2.7 s_{C^*} 89.3 (0.091) s_A 111.5 (1.09) i i 104.9 (−1.06) s_A 84.9 (−0.079) s_{C^*} 0.2 g
C8/C**	g 5.86 s_{C^*} 84.0 (0.175) s_A 92.3 (0.867) i i 84.9 (−0.818) s_A 79.1 (−0.146) s_{C^*} 2.23 g
C6/C**	g 13.4 s_X 40.1 (0.184) s_{C^*} 84.8 (1.08) i i 75.4 (−1.06) s_{C^*} 36.5 (−0.021) s_X 5.78 g

[a] Listed are 2nd heating and 1st cooling data.

pression Teflon trough was used with a compression speed between 0.2 and 50 Å^2/repeat unit·min (typically ≈ 3 Å^2/repeat unit·min, unless otherwise noted). The subphase used was purified water (18-MΩ resistivity) using a Milli-Q water system (Millipore). All measurements were made at 27 °C unless otherwise noted. The solutions were spread on the water surface from a microsyringe (Hamilton, gas tight) prior to compression. Surface pressure was measured using the Wilhelmy plate method. Surface areas are expressed as mean molecular area per monomer repeat unit of the polymer. Surface potentials were measured with the vibrating plate method. The monolayer stability was measured by monitoring the isobaric creep, the change in mean molecular area at constant applied surface pressure. Hysteresis measurements were made with compression speeds of order 3 Å^2/repeat unit·min and expansion speeds of order 0.2 Å^2/repeat unit·min. It was important to use two symmetric compression barriers with the Wilhelmy plate placed in the middle of the trough facing parallel to the moving barriers for reproducible results on these polymers. Because the polymer monolayers were viscous at high applied surface pressures, erroneous data were easily induced due to the deflection of the Wilhelmy plate if one barrier was used. All isotherms were run a minimum of three times, with reproducibility errors of less than ±1 Å^2.

Surface UV-visible spectra were obtained by a modified Instaspec 2 cooled diode array spectrophotometer system from Oriel Corp. mounted over the Langmuir trough and a xenon arc lamp source for illumination. Spectra were obtained during compression by a single reflection technique with a focusing mirror in the subphase. Quartz fiber lightguides were used between the light source and monolayer and the monolayer and spectrophotometer. A Uniblitz computer-controlled shuttering system was also used with the xenon source to minimize potential radiation damage to the monolayer. Spectra were integrated for 0.3 s with a 15-s delay between acquisitions.

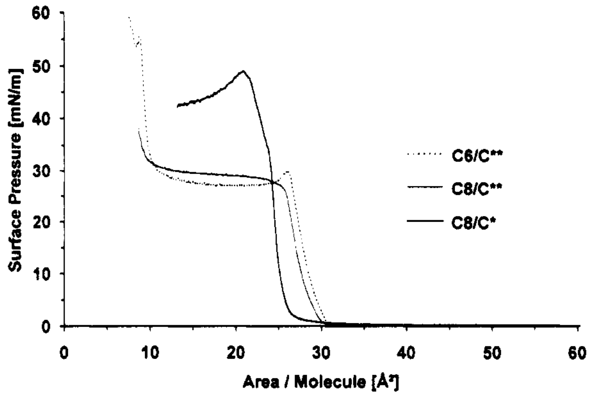

Figure 1. Surface pressure vs mean molecular area isotherms of the three polymers.

Results and Discussion

The mesomorphic behavior of these polymers is presented in Table I. Both C8/C* and C8/C** exhibit enantiotropic s_{C^*} and s_A phases. C6/C** exhibits an enantiotropic s_{C^*} phase and an unidentified smectic (s_X) phase. The s_{C^*} phase of all three polymers is stable from room temperature, i.e., just above the glass transition temperature up to about 85 °C, except for the case of C6/C** which has a s_X phase up to 40 °C. All three polymers form fluid birefringent melts in the disordered smectic phase. Therefore, the side-chain nature, wide s_{C^*} phase range and bulk fluidity of these polymers make them ideal candidates for studies as Langmuir films near room temperature.

Isotherms. Figure 1 shows the isotherms of the investigated polymers. All three polymers showed a monotonic increase in the surface pressure with decreasing surface area and collapse pressures in the range of 27–49 mN/m. Extrapolation of the isotherms to zero pressure leads to lower mean molecular area (25.7 Å^2) for the polymer C8/C* compared to C6/C** (30 Å^2) and that of C8/C** (28.5 Å^2). These isotherms have the typical shape for condensed polymer monolayers except for a tail in the pressure onset region of C8/C* which may indicate an expanded phase as well or may be an effect of the polymer backbone compressibility.[42] Above 5 mN/m, the slopes of the isotherms of all three polymers are similar. This might suggest that the packing of the mesogenic groups in the monolayer is similar[39] and not highly dependent on the length of the alkyl side chain. The mean molecular areas of the three polymers at collapse 21, 25.5, and 26.7 Å^2 for C8/C*, C8/C**, and C6/C** respectively, are similar to those seen in bulk smectic liquid crystalline phases and suggest that the limiting packing area at high applied surface pressures is determined by the mesogens. The lower area seen in the C8/C* sample is probably due to slightly between packing possible with a single chiral center. The higher apparent collapse point observed with the C8/C** material may also arise from closer packing and is further discussed below. The isotherm reproducibility with all polymers under identical conditions was better than 1 mN/m at a given surface area. Slightly larger differences could be observed near the collapse pressure.

Temperature-dependent isotherms of C8/C* and C8/C** are shown in parts a and b of Figure 2, respectively. These measurements show only a small temperature influence on the packing behavior of the polymers. This also indicates that the packing is dominated by the mesogens, as a larger temperature effect would be expected from the backbone. The collapse pressure, for all three polymers, however, decreases significantly with increasing temperature.

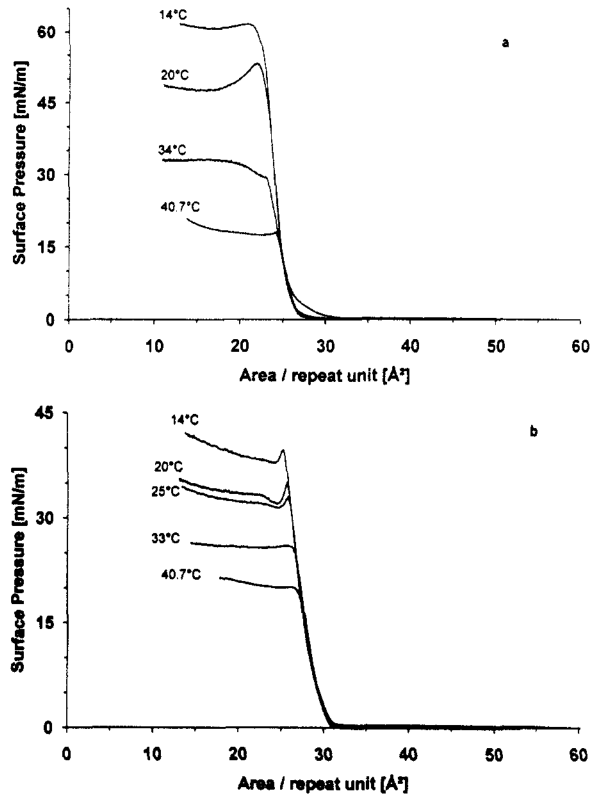

Figure 2. (a) Temperature dependence of surface pressure isotherms of C8/C*. (b) Temperature dependence of surface pressure isotherms of C8/C**.

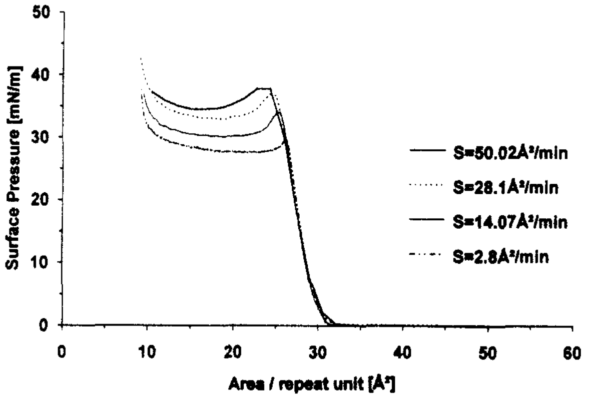

Figure 3. Compression rate dependence of surface pressure isotherms of C8/C**.

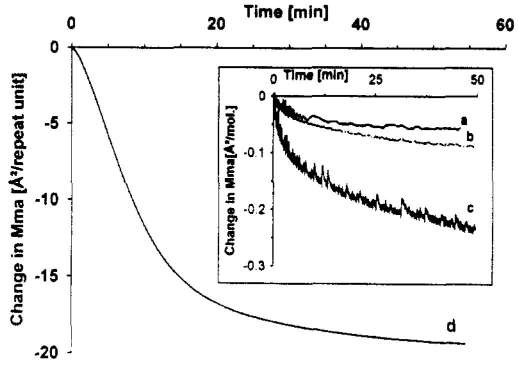

Figure 4. Applied surface pressure (π) dependence of the isobaric creep in C6/C**. Inset curves: (a) π = 5 mN/m, (b) π = 1-mN/m, (c) π = 15 mN/m. Large curve: (d) π = 26 mN/m.

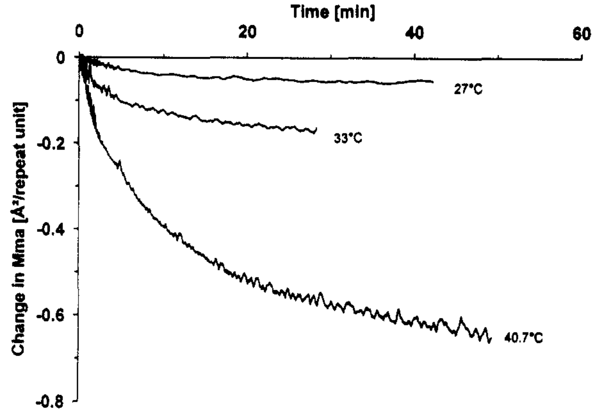

Figure 5. Temperature dependence of the isobaric creep of C8/C** at π = 10 mN/m.

Figure 3 shows the isotherms of the C8/C** polymer at different compression rates. All the polymers showed similar rate dependence in that no significant change in the onset mean molecular area was observed, but the collapse pressure dropped significantly with the compression rate, especially in the case of C6/C** and C8/C*. This large change in the collapse pressure with both temperature and compression rate may be indicative that the compounds exhibit a viscoelastic component to the measured surface pressure, probably due to the polymer backbone. Different authors have already reported this type of behavior in the literature.[46-48] It has sometimes been discussed as a rollover collapse of the mesogens lying flat on the surface. This interpretation cannot be applied to our measurements because the mean molecular area at the onset pressure of all the polymers under study is far too small for all the molecules to be lying flat on the surface. Sometimes it has been interpreted in terms of a collapse process which is much slower than the compression rate, thus leading to a metastable phase. It has also been discussed as an expulsion of the repeat units out of the monolayer to form local bilayer regions.[42,49,50] Other possibilities could be simply a crystallization of the monolayer into the bulk or dissolution into the subphase. In fact these polymers, as is discussed below, tended to show reversible collapse, and this might support the idea of local bilayer formation and a large surface viscosity at high pressures.

Stability. Isobaric creep tests are considered to be important basic experiments to study the stability of the monolayer at the air/water interface. In general, all three compounds showed very good stability (less than 1-Å² creep over 60 min) at pressures below the surface pressure isotherm inflection point. Figure 4 shows the behavior of the C6/C** polymer at applied surface pressures of 5, 10, 15, and 26 mN/m. At pressures below the inflection point of the surface pressure isotherm (curves a–c), the monolayer was very stable. At pressures above the inflection point, however, the monolayer relaxed considerably, creeping to an area of about 10 Å² which may indicate multilayer formation. All the polymers showed similar behavior at surface pressures above the isotherm inflection point. Stability measurements were also done at different temperatures. Figure 5 shows the increase in the isobaric creep of the C8/C** polymer with increasing temperature. This behavior is representative of that observed in all the compounds at pressures below the isotherm inflection point and indicates the films are reasonably stable even at subphase temperatures as high as 40.7 °C over short times. The relatively small temperature dependence of the creep also indicates that the polymers are not dissolving in the subphase.

Hysteresis. Hysteresis measurements done by following successive compression and expansion cycles show reversible behavior of all polymers below their respective collapse pressure. Typical examples are shown in parts

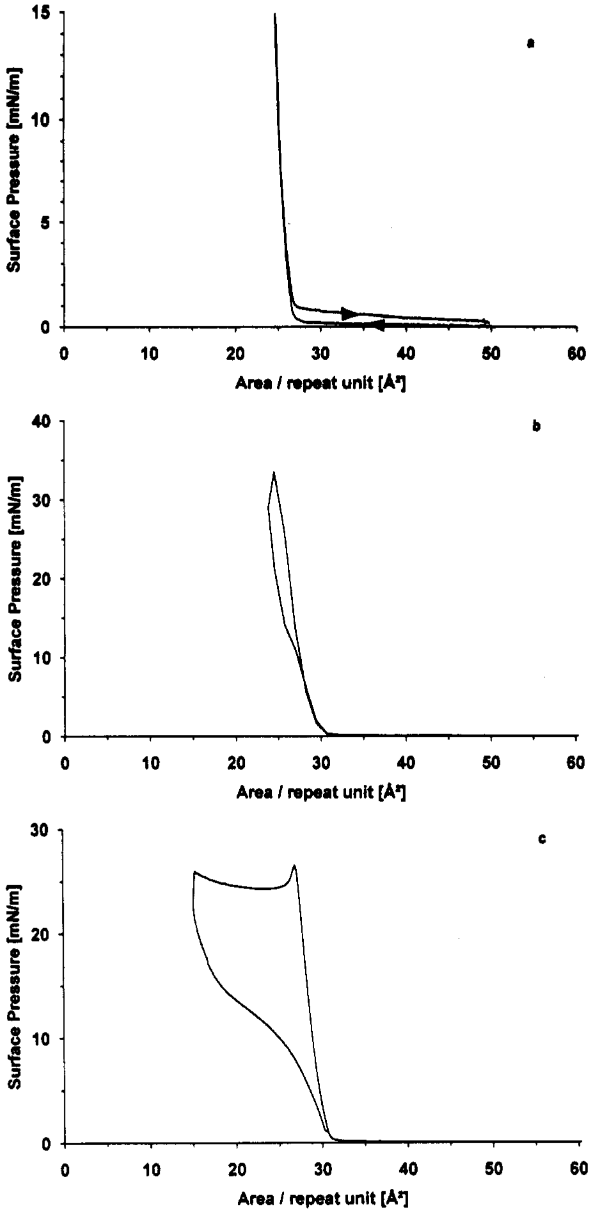

Figure 6. Hysteresis of the surface pressure isotherm: (a) C8/C* compressed below the collapse point. Note: the small positive shift in the measured surface pressure on expansion at high surface areas results from a small amount of polymer adhering the platinum Wilhelmy plate used in these experiments. (b) C8/C** compressed just to the apparent collapse point. (c) C6/C** compressed beyond its apparent collapse point.

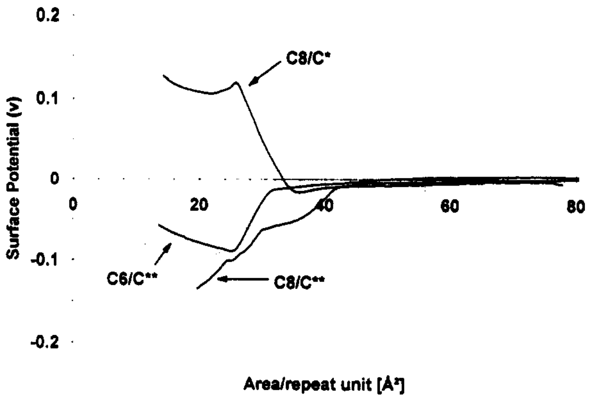

Figure 7. Surface potential vs surface area isotherms of the three polymers.

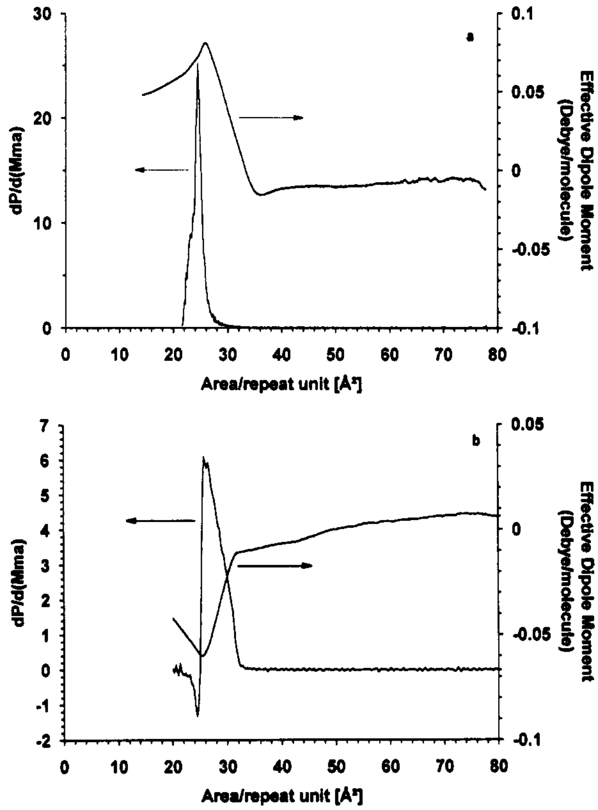

Figure 8. Effective dipole moment and derivative of surface pressure with respect to surface area vs mean molecular area of (a) C8/C* and (b) C6/C**.

a–c of Figure 6. All the polymers showed complete reversibility when compressed and expanded below the collapse point as shown in Figure 6a. They also showed a tendency toward reversible collapse as shown in parts b and c of Figure 6 in that the expansion curves tended to rejoin the compression curves at low surface pressures. Polymers C6/C** and C8/C** did not show complete reversible collapse in that subsequent compressions of the same monolayer showed shifts of the isotherms toward lower surface areas, suggesting an irreversible collapse. This behavior may well have been due to small amounts of the polymer creeping under the trough barrier or a small amount of irreversible bilayer crystallization.

Surface Potential. Generally, the surface potential during the formation of a monolayer has been observed to increase with increasing compression and does not necessarily follow the curve of the isotherm.[35,36,51] It is defined as the change in the potential across the water/air interface and is proportional to the interfacial change in the normal component of the dipole moment density as described by the Helmholtz equation[35,36,52,53]

$$\Delta\mu = \epsilon \Delta V A$$

where $\Delta V = V_m - V_{w-a}$ is the measured surface potential (V_m is the surface potential of the air/monolayer/water interfaces and V_{w-a} is the surface potential of the clean air/water interface), ϵ is the vacuum permitivity, and A is the measured area per repeat.

The surface potential measurements of the polymers studied in this work showed different behavior and are summarized in Figure 7. The calculated dipole moments for C8/C* and C6/C** are shown in parts a and b of Figure 8, respectively, along with the derivative of the surface pressure with respect to the surface area. The C8/C* polymer exhibited a linear change in the dipole moment (Figure 8a) starting at about 35 Å^2 up to a maximum corresponding to a mean molecular area of 25.5 Å^2. The surface pressure inflection point calculated from the derivative of the surface pressure with respect to the Mma

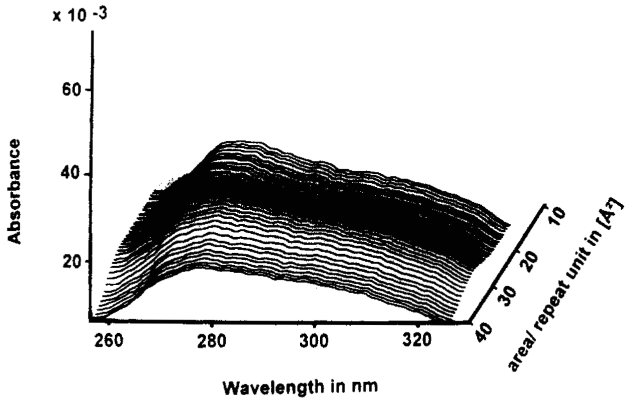

Figure 9. UV-visible spectra of a C8/C** monolayer at the air/water interface during compression.

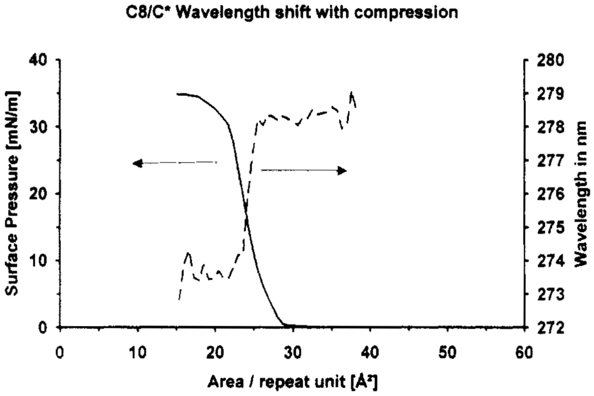

Figure 10. λ_{max} (dashed line) and surface pressure (solid line) vs surface area of the C8/C** polymer.

corresponds to a value of about 24.5 Å^2 on the Mma axis. This result suggests that the change in the molecular orientation toward that of the close-packed monolayer starts at about 35 Å^2, in other words, before the surface pressure is measurably changing. The rather extended surface pressure onset in this polymer, however, may be due to orientation of the mesogens. The surface potential results also indicate the maximal orientation is reached at areas of about 25.5 Å^2, very near the inflection point of the pressure isotherm. The fact that the dipole moment decreases slowly at surface areas smaller than its maximum value suggests that the monolayer entered into its collapse phase and is consistent with local bilayer formation.

The two other LC substances, C8/C** and C6/C**, show the presence of a negative change in the dipole moment as shown in Figure 8b for C6/C**. The change in the polarity at the water/air interface is consistent with that resulting from a negative total dipole moment or one directed from the monolayer (−) to the water (+)[51] which could be explained if in one polymer the side chains pointed toward the water surface and in the other they pointed away. As shown in Scheme I though, the chemical difference between the two sets of polymers is not sufficient to change their amphiphilicity such that this change in orientation is likely. If it is assumed that the side chains point toward the water surface, however, the surface potential differences can be explained in terms of the hydration shell. It is well-known that, in addition to the monolayer's surface potential contribution, one can have a strong contribution from the dipoles of the water molecules at the water/monolayer interface.[51] In this case, the presence (C6/C** and C8/C**) or absence (C8/C*) of the electronegative chlorine atom at the end of the mesogen may be sufficient to change the hydration shell such that the potential of the water molecules at the interface dominates the measured surface potential. It should also be noted that, in the above case, the meaning of the calculated effective dipole moment is changed considerably. Nonetheless, knowledge of the surface potential behavior of such polymers may prove useful in understanding their switching behavior in very thin films and the bulk.

Surface UV-Visible Spectroscopy. Surface UV-vis measurements were performed on all three polymers with a view toward obtaining additional information on the intermolecular interactions of the mesogens. Figure 9 shows the spectra obtained during the compression of the C8/C* polymer. Three features are apparent upon inspection.

First, there is an increase in the absorption with decreasing surface area. This is primarily due to increasing the polymer surface concentration as the illuminating beam had a constant spot size. This behavior was observed with all three polymers.

Second, a hypsochromic shift is seen in the λ_{max} of the peak located at about 280 nm. Figure 10 illustrates how the λ_{max} correlated with the surface pressure. Unlike the surface potential, the onset of the λ_{max} shift occurs after the surface pressure onset. This indicates that the mesogens are only well orientationally ordered at relatively high applied surface pressures. No λ_{max} shift was observed for both C8/C** and C6/C**, indicating that the somewhat bulkier mesogen in these polymers impedes high orientational order.

Third, at low surface areas, a shoulder appears at about 290 nm. The assignment of this absorbance is unknown.

In summary, all three polymers investigated spread to form stable monolayers at the air/water interface. Isotherm measurements and surface potential indicate that the mesogens are oriented during compression, becoming closer packed, and oriented toward the water surface at high pressures. Mesogen–mesogen interactions and packing seemed to account for many of the observed differences in the monolayer behavior rather than the backbones. A systematic study of such polymers confined to monolayers at free surfaces may be of use in tailoring bulk properties as well. Both the hysteresis and stability behavior of all three polymers indicate that they may be ideal candidates for dipping on solid substrates. Transfer of preformed polymer films[54] to appropriate substrates can avoid structural defects like those observed with the irradiation polymerization of unsaturated monomeric Langmuir–Blodgett layers.[55,56] Analysis by small-angle X-ray diffraction should reveal the stacking structure of the deposited multilayers. Different spectroscopic analyses, such as spontaneous polarization, switching, and phase behavior experiments are also necessary to complete the study of Langmuir–Blodgett monolayer and multilayer behavior of these polymers.

Acknowledgment. Financial support by the Office of Naval Research, the Bio/Molecular Science and Engineering group of the NRL, and donors to the Petroleum Research Fund as administered by the ACS is gratefully acknowledged. Technical assistance from KSV Instruments, Helsinki, and the Oriel Corp. is also acknowledged.

References and Notes

(1) Goodby, J. W. *J. Mater. Chem.* **1991**, *1*, 307.
(2) Walba, D. M.; Keller, P.; Parmar, D. S.; Clarck, N. A.; Wand, M. D. *J. Am. Chem. Soc.* **1989**, *111*, 8273.
(3) Goodby, J. W.; Waugh, M. A.; Stein, S. M.; Chin, E.; Pindak, R.; Patel, J. S. *J. Am. Chem. Soc.* **1989**, *111*, 8119.
(4) Walba, D. M.; Slater, C. S.; Thurmes, W. N.; Clark, N. A.; Handsky, M. A.; Supon, F. *J. Am. Chem. Soc.* **1986**, *108*, 5210.

(5) Levelut, A. M. *J. Phys. (Paris)* **1983**, *44*, 623.

(6) Takanishi, Y. J. *J. Appl. Phys.* **1991**, *30*, 2023.

(7) Goodby, J. W.; Bline, R.; Clark, N. A.; Lagerwall, S. T.; Osipov, M. A.; Pikin, S. A.; Sakurnai, T.; Yoshino, K.; Zeks, B. In *Ferroelectric Liquid Crystals, Principles Properties and Applications*; Gordon and Breach Science Publishers: New York, 1991.

(8) LeBarny, P.; Dubois, J. C. In *Side Chain Liquid Crystal Polymers*; McArdle, C. B., Ed.; Chapman and Hall: New York, 1989; p 130.

(9) Goodby, J. W. *Science (Washington, D.C.)* **1986**, *231*, 350.

(10) Goodby, J. W.; Leslie, T. M. *Mol. Cryst. Liq. Cryst.* **1989**, *114*, 151.

(11) Barbera, J.; Omenat, A.; Serrano, J. L. *Mol. Cryst. Liq. Cryst.* **1989**, *166*, 167.

(12) Otterholm, B.; Nilsson, M.; Lagerwall, S. T.; Skarp, K. *Liq. Cryst.* **1987**, *2*, 757.

(13) Bradshaw, M.; Constant, J.; Raynes, E. Annual Conference of the British Liquid Crystal Society, Manchester, U.K., 1986.

(14) LeBarny, P.; Dubois, J. C. In *Side Chain Liquid Crystal Polymers*; McArdle, C. B., Ed.; Chapman and Hall: New York, 1989; p 260.

(15) Wendorff, J. H. *Angew. Chem., Int. Ed. Engl.* **1991**, *30*, 405.

(16) Tieke, B. *Adv. Mater.* **1990**, *2*, 222.

(17) Bualek, S.; Kapitza, H.; Meyer, J.; Schmidt, G. F.; Zentel, R. *Mol. Cryst. Liq. Cryst.* **1988**, *155*, 47.

(18) Percec, V.; Pugh, C. In *Side Chain Liquid Crystal Polymers*; McArdle, C. B., Ed.; Chapman and Hall: New York, 1989; p 30.

(19) Goodby, J. W.; Waugh, M. A.; Stein, S. M.; Chin, B.; Pindak, R.; Patel, J. S. *J. Am. Chem. Soc.* **1989**, *111*, 8119.

(20) Blinov, L. M.; Baikalov, V. A.; Barnik, M. J.; Beresnev, L. A.; Pozhidayev, B. P.; Yablonsky, S. V. *Liq. Cryst.* **1987**, *2*, 121.

(21) Decobert, G.; Dubois, J. C.; Essenlin, S.; Noel, C. *Liq. Cryst.* **1986**, *1*, 307.

(22) Esselin, S.; Bosios, L.; Noel, C.; Decobert, G.; Dubois, J. C. *Liq. Cryst.* **1987**, *2*, 505.

(23) Esselin, S.; Noel, C.; Decobert, G.; Dubois, J. C. *Mol. Cryst. Liq. Cryst.* **1988**, *155*, 371.

(24) Zentel, R.; Reckert, G.; Reck, B. *Liq. Cryst.* **1987**, *2*, 84.

(25) Bualek, S.; Zentel, R. *Makromol. Chem.* **1988**, *189*, 797.

(26) Vallerien, S. U.; Zentel, R.; Kremer, F.; Kapitza, H.; Fischer, E. W. *Makromol. Chem., Rapid Commun.* **1989**, *10*, 333.

(27) Zentel, R.; Kapitza, H.; Kremer, F.; Vallerien, S. U. In *Liquid Crystalline Polymers*; Weiss, R. A., Ober, C. K., Eds.; ACS Symposium Series 435; American Chemical Society: Washington, DC, 1990; p 207.

(28) Endo, H.; Hachiya, S.; Uchida, S.; Hashimoto, K.; Kawasaki, K. *Liq. Cryst.* **1991**, *9*, 635.

(29) Koide, N.; Uehara, K.; Limura, K. *Mol. Cryst. Liq. Cryst.* **1988**, *157*, 151.

(30) Suzuki, T.; Okawa, T.; Ohnuma, K.; Sakon, Y. *Makromol. Chem., Rapid Commun.* **1988**, *9*, 755.

(31) Dumon, M.; Nguyen, H. T.; Mauzac, M.; Destrade, C.; Achard, M. F.; Gasparoux, H. *Macromolecules* **1990**, *23*, 355.

(32) Percec, V.; Wang, C. S. *J. Macromol. Sci., Chem.* **1992**, *A29*, 99.

(33) Clark, N. A.; Lagerwall, S. *Appl. Phys. Lett.* **1980**, *36*, 899.

(34) Kremer, F.; Vallerien, S. U. In *Liquid Crystalline Polymers*; Weiss, R. A., Ober, C. K., Eds.; ACS Symposium Series 435; American Chemical Society: Washington, DC, 1990; p 207.

(35) Gaines, G. L., Jr. *Insoluble Monolayers at the Gas–Water Interface*; Wiley-Interscience; New York, 1966.

(36) Roberts, G., Ed. Langmuir-Blodgett *Films*; Plenum Press: New York, 1990.

(37) Pfieffer, S.; Adams, J.; Duran, R. S.; Shashidhar, R. *Appl. Phys. Lett.*, in press.

(38) Rettig, W.; Naciri, J.; Shashidhar, R.; Duran, R. S. *Thin Solid Films* **1992**, *210*, 114.

(39) Rettig, W.; Naciri, J.; Shashidhar, R.; Duran, R. S. *Macromolecules* **1991**, *24*, 6539.

(40) Adams, J.; Thibodeaux, A. F.; Naciri, J.; Shashidhar, R.; Duran, R. S. *Polym. Prepr. (Am. Chem. Soc., Div. Polym. Chem.)* **1992**, *31*, 1164.

(41) Adams, J.; Rettig, W.; Shashidhar, R.; Naciri, J.; Duran, R. S. *J. Phys. Chem.*, in press.

(42) Adams, J.; Buske, A.; Duran, R. S. *Macromolecules*, in press.

(43) Percec, V.; Zheng, Q.; Lee, M. *J. Mater. Chem.* **1991**, *1* (6), 1015.

(44) Percec, V.; Zheng, Q. *J. Mater. Chem.* **1992**, *2*, 475.

(45) Percec, V.; Zheng, Q. *J. Mater. Chem.*, in press.

(46) Diep-Quang, H.; Ueberreiter, K. *Polymer* **1981**, *13*, 623.

(47) Kato, T. *Langmuir* **1990**, *6*, 870.

(48) Kato, T.; Hirobe, Y.; Kato, M. *Langmuir* **1991**, *7*, 2208.

(49) Rapp, B.; Gruler, H. *Phys. Rev. A* **1990**, *42*, 2215.

(50) Rapp, B.; Eberhardt, M.; Gruler, H. *Makromol. Chem., Macromol. Symp.* **1990**, *46*, 439.

(51) Vogel, V.; Mobius, D. *Thin Solid Films* **1988**, *159*, 73.

(52) Davies, J. T.; Rideal, E. K. *Interfacial Phenomena*, 2nd ed.; Academic Press: New York, 1963.

(53) Tredgold, R. H. *Thin Solid Films* **1987**, *152*, 223.

(54) Embs, F.; Funhoff, D.; Laschewsky, A.; Licht, U.; Ohst, H.; Prass, W.; Ringsdorf, H.; Wegner, G.; Wehrmann, R. *Adv. Mater.* **1991**, *3*, 25.

(55) Day, D.; Lando, J. B. *Macromolecules* **1980**, *13*, 1478.

(56) Naegele, D.; Ringsdorf, H.; Tieke, B.; Wegner, G.; Day, D.; Lando, B. *Chem.-Ztg.*, **1976**, *10*, 426.